

Measurements of the Thermal Conductivity of HFC-143a in the Temperature Range from 300 to 500 K at Pressures up to 50 MPa¹

B. Le Neindre,^{2,3} Y. Garrabos,⁴ and M. S. Kim⁵

Received June 26, 2000

Measurements of the thermal conductivity of HFC-143a that were made by a coaxial cylinder cell operating in steady state are reported. The measurements of the thermal conductivity of HFC-143a were performed along several quasi-isotherms between 300 and 500 K in the gas and liquid phases. The pressure range covered varies from 0.1 to 50 MPa. Based on the measurement of more than 600 points, an empirical equation is provided to describe the thermal conductivity outside the critical region as a function of temperature and density. A careful analysis of the various sources of error leads to an estimated uncertainty of approximately $\pm 1.5\%$.

KEY WORDS: coaxial cylinders; HFC-143a; high pressure; refrigerants; thermal conductivity.

1. INTRODUCTION

Recently the thermophysical properties of HFC-143a (1,1,1-trifluoroethane) were investigated widely since this hydrofluorocarbon, in combination with pentafluoroethane (HFC-125) and/or 1,1,1,2-tetrafluoroethane (HFC-134a), is expected to be an environmentally acceptable alternative to the refrigerant HCFC-22 (chlorodifluoromethane) used in refrigeration, heat pumps, and

¹ Paper presented at the Fourteenth Symposium on Thermophysical Properties, June 25–30, 2000, Boulder, Colorado, U.S.A.

² LIMHP-CNRS, Institut Galilée, Université Paris Nord, Av. J. B. Clément, 93430 Villetaneuse, France.

³ To whom correspondence should be addressed. E-mail: leneindr@limhp.univ-paris13.fr

⁴ Institut de Chimie de la Matière Condensée de Bordeaux, Université de Bordeaux 1, Av. du Dr. Schweitzer, 33608 Pessac, France.

⁵ Department of Mechanical Engineering, Seoul National University, Seoul 151-742, Korea.

air-conditioning equipment. There are very few measurements of the transport properties of HFC-143a compared to other refrigerants. The thermal conductivity of HFC-143a was measured in a vertical coaxial cylinder cell, operating in the steady-state mode. We have studied the influence of temperature and pressure on the thermal conductivity. The measurements were performed to make an analysis of the data based on the residual concept. The thermal conductivity $\lambda(T, \rho)$ as a function of temperature T and density ρ may be represented as the sum of three terms:

$$\lambda(T, \rho) = \lambda_0(T) + \Delta\lambda(T, \rho) + \Delta\lambda_c(T, \rho) \quad (1)$$

where $\lambda_0(T)$ is the dilute gas thermal conductivity, $\Delta\lambda(T, \rho)$ is the residual thermal conductivity, and $\Delta\lambda_c(T, \rho)$ is the critical enhancement. The dilute-gas contribution $\lambda_0(T)$ was obtained by performing measurements at atmospheric pressure as a function of temperature. The background term,

$$\lambda_B(T, \rho) = \lambda_0(T) + \Delta\lambda(T, \rho) \quad (2)$$

was obtained by making measurements along quasi-isotherms as a function of pressure in the liquid and gas phases far away from the critical region. The remaining contribution, $\Delta\lambda_c(T, \rho)$, represents the enhancement of the thermal conductivity due to critical fluctuations and becomes significant in the supercritical region or in the subcritical region along the saturation curve. In this paper, we report only experimental data in the liquid and gas phases far away from the critical point to determine the so-called thermal conductivity background. Our measurements in the critical region and in the gas phase below the critical point will be reported later. The density was calculated with the equation of state reported by Outcalt and McLinden [1], where the critical parameters are given as follows: $T_c = 346.04$ K, $p_c = 3.7756$ MPa, and $\rho_c = 432.9$ kg · m⁻³.

2. EXPERIMENTAL APPARATUS

The thermal conductivity of HFC-143a was measured using vertical coaxial cylinders operating in the steady-state mode. The same device was used in the measurement of the thermal conductivity of 1-chloro-1,1-difluoroethane (HCFC-142b) [2], pentafluoroethane (HFC-125) [3], and 1,1,1,2-tetrafluoroethane (HFC-134a) [4]. A detailed description of the cell and of the measurement method is available elsewhere [5]. The sample was provided by Elf-Atochem, and its purity was estimated to be better than 99.5% by the manufacturer's analysis.

3. DILUTE-GAS THERMAL CONDUCTIVITY

The results of the measurement of the thermal conductivity at atmospheric pressure are listed as a function of temperature in Table I. The experimental data were fitted by a linear equation,

$$\lambda_0 = -18.59 + 0.10723T \quad (3)$$

where λ_0 is given in $\text{mW} \cdot \text{m}^{-1} \cdot \text{K}^{-1}$ and T in K.

Table I. The Thermal Conductivity of HFC-143a at Atmospheric Pressure

T (K)	λ ($\text{mW} \cdot \text{m}^{-1} \cdot \text{K}^{-1}$)
299.17	13.62
301.96	13.83
302.29	13.86
306.79	14.38
307.45	14.48
309.33	14.57
311.74	14.82
324.25	16.03
324.55	16.08
327.58	16.43
328.63	16.51
329.08	16.53
335.10	17.42
340.88	18.17
342.63	18.29
343.22	18.36
343.24	18.15
353.40	19.09
355.89	19.73
356.75	19.61
356.76	19.43
377.02	21.85
377.26	21.70
377.29	21.74
396.28	24.18
407.57	24.96
416.02	25.72
435.05	27.99
454.71	30.15
474.42	32.23
484.42	33.61
499.02	34.95

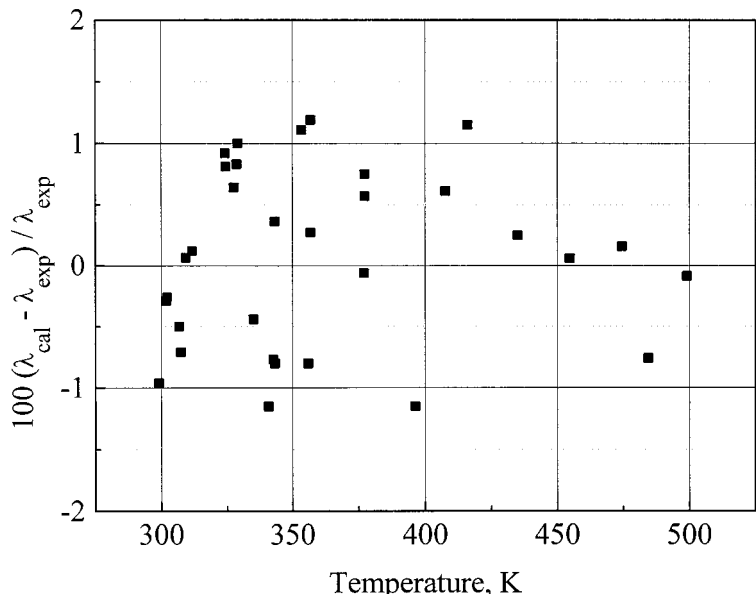


Fig. 1. Relative deviations between the calculated values of thermal conductivity [Eq. (3)] and experimental data from this work at atmospheric pressure.

Figure 1 shows the deviations between our experimental data measured at atmospheric pressure and Eq. (3); the data are within 1.5%, which is always smaller than the experimental uncertainties. Figure 2 shows the deviations of the data of Hammerschmidt [6] and Tanaka et al. [7] from Eq. (3). The corresponding values calculated by Eq. (3) are larger than their data and increase with an increase in temperature; they reach 18% at 418 K and 13% at 353 K.

The temperature dependence of the thermal conductivity of the dilute gas can be represented by an expression derived from the kinetic theory of gases. The thermal conductivity is related to the reduced effective collision cross sections that contain all the contributions of translational, rotational, vibrational, and electronic degrees of freedom. As there is a lack of reliable experimental data on the vibrational collision number, for the calculation of the thermal conductivity in the zero density, we used the practical engineering form:

$$\lambda_0(T) = \frac{0.177568(T/M)^{0.5} C_P^0 / R}{\sigma^2 \Omega_\lambda^*(T^*)} \quad (4)$$

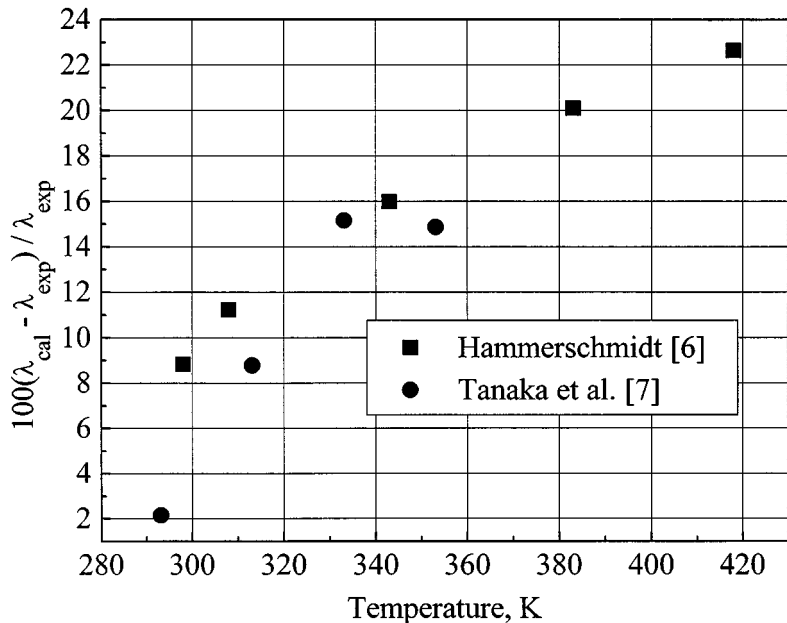


Fig. 2. Relative deviations of calculated values of thermal conductivity by [Eq. (3)] from experimental data at atmospheric pressure.

where M is the molar mass in $\text{kg} \cdot \text{kmol}^{-1}$, T is the absolute temperature, $\Omega_i^*(T^*)$ is the reduced effective collision cross section for thermal conductivity, C_P^0 is the ideal isobaric heat capacity, and R is the gas constant. The reduced temperature is given by $T^* = kT/\varepsilon$, where k is Boltzmann's constant.

The scaling factors σ and ε/k , which correspond to the effective Lennard-Jones 12–6 potential parameters, were determined by a regression analysis of both viscosity and thermal conductivity data at atmospheric pressure. For this purpose the experimental viscosity data (in $\mu\text{Pa} \cdot \text{s}$) of Takahashi et al. [8] near atmospheric pressure were represented by the linear equation:

$$\eta_0 = -0.1644 + 0.03829T \quad (5)$$

where T is in K. They were compared to the low-pressure gas viscosity given by the Chapman-Enskog equation derived from the kinetic theory of gases:

$$\eta_0(T) = \frac{0.026693(TM)^{0.5}}{\sigma^2 \Omega_\eta^*(T^*)} \quad (6)$$

where $\Omega_\eta^*(T^*)$ is the reduced effective collision cross section for viscosity. Some authors consider a high-order correction factor for thermal conductivity f_λ and viscosity f_η . In fact, we have found that the inclusion of these terms does not significantly improve the fits and complicate the analysis of the data.

To carry on the calculations, the ideal specific heat at constant pressure was calculated from the data reported by Yokozeki et al. [9]:

$$\frac{C_P^0}{R} = \sum_{i=0}^6 c_i T^i \quad (7)$$

where

$$\begin{aligned} c_0 &= 2.912897, & c_1 &= 1.448316 \times 10^{-2}, & c_2 &= 6.678891 \times 10^{-5} \\ c_3 &= -8.24828 \times 10^{-7}, & c_4 &= 2.663593 \times 10^{-10} \\ c_5 &= -1.668859 \times 10^{-13}, & c_6 &= 4.189036 \times 10^{-17} \end{aligned}$$

and $R = 8.314471 \text{ J} \cdot \text{mol}^{-1} \cdot \text{K}^{-1}$.

The reduced collision integral Ω_λ^* was estimated as a function of reduced temperature, $T^* = kT/\varepsilon$, using the functional expansion:

$$\Omega_\lambda^* = \sum_{j=1}^3 A_j (1/T^*)^j \quad (8)$$

where

$$A_1 = 0.444358, \quad A_2 = 0.327867, \quad A_3 = 0.1936835$$

For the collision integral of the viscosity, we used the following equation reported by Kestin et al. [10]:

$$\Omega_\eta^* = \exp \left[0.46641 + \sum_{j=1}^4 B_j \ln(T^*)^j \right] \quad (9)$$

where

$$\begin{aligned} B_1 &= -0.56991, & B_2 &= 0.19591 \\ B_3 &= -0.03879, & B_4 &= 0.00259 \end{aligned}$$

The best agreement between experimental data on thermal conductivity and viscosity and calculated values by the corresponding theoretical

equations [Eqs. (4) and (6)] was found for $\varepsilon/k = 298$ K and $\sigma = 0.480$ nm. The average deviations are of the order of $\pm 2.5\%$ in the respective temperature ranges of the experiments, except near room temperature, where the application of the theory is questionable for the thermal conductivity. In fact, it is always feasible to improve the agreement between experimental data and corresponding values calculated by theoretical equations. For viscosity, for instance, with the set of potential parameters $\varepsilon/k = 290$ K and $\sigma = 0.4885$ nm, the maximum deviation is less than $\pm 0.5\%$, but for thermal conductivity the maximum deviation increases up to $\pm 6\%$. The analysis of the transport properties at atmospheric pressure of the refrigerants that we have studied up to now leads to the same conclusion. It is possible to calculate the thermal conductivity and the viscosity at a low density using Chapman-Enskog equations and the appropriate potential parameters with an average deviation of the order of $\pm 2.5\%$ with respect to the experimental data. The relative deviations of the present experimental thermal conductivity data from their optimal representation by Eqs. (4), (7), and (8) are shown in Fig. 3. The relative deviations between the calculated values of viscosity [Eqs. (6) and (9)] and the data of Takahashi et al. [8] are shown in Fig. 4. The percentage deviations between theoretical thermal conductivity values calculated by Eqs. (4), (7), and (8) and calculated data

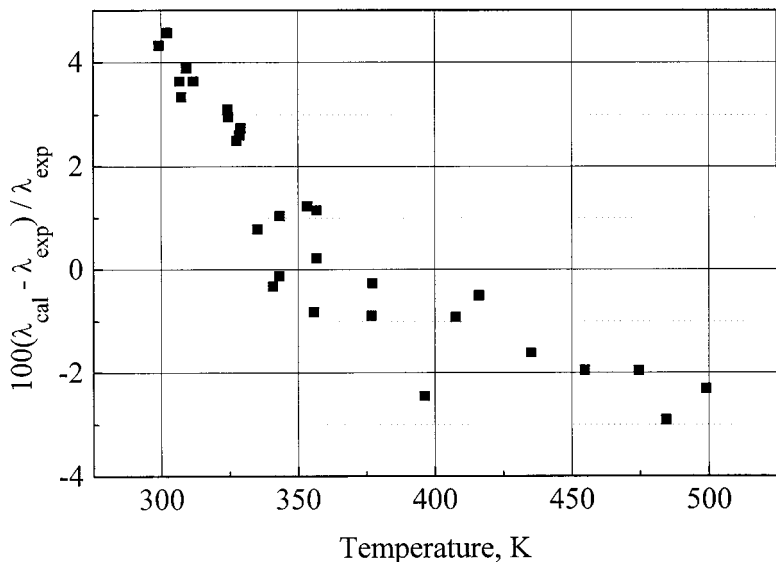


Fig. 3. Relative deviations between theoretical calculated values of thermal conductivity [Eqs. (4), (7), and (8)] and experimental data from this work at atmospheric pressure.

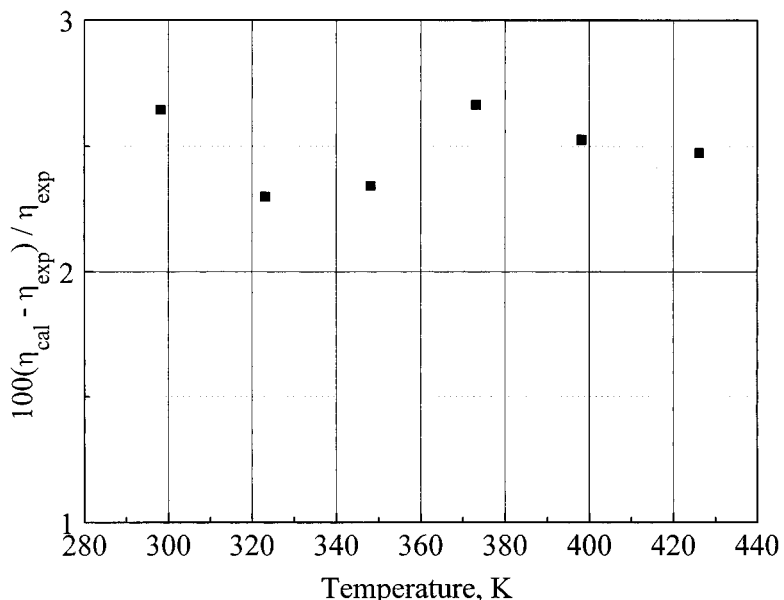


Fig. 4. Relative deviations between theoretical calculated values of viscosity [Eqs. (6) and (9)] and experimental data of Takahashi et al. [8] at atmospheric pressure.

Table II. Thermal Conductivity of HFC-143a Along the Quasi-Isotherm 306.3 K

Temperature (K)	Pressure (MPa)	Density (kg · m ⁻³)	λ (mW · m ⁻¹ · K ⁻¹)
307.13	0.55	19.8	14.57
306.63	0.541	19.5	14.68
306.46	1.05	42.2	14.86
305.62	1.044	42.2	15.29
305.62	1.145	47.5	15.33
305.62	1.184	49.6	15.36
305.61	1.191	50.0	15.40
305.61	1.260	54.0	15.48
305.60	1.291	55.8	15.54
305.60	1.303	56.5	15.57
305.60	1.365	60.4	15.62
305.10	1.371	61.0	15.73
305.10	1.382	61.7	15.86
305.09	1.383	61.8	15.94
305.09	1.384	61.9	15.99
304.92	1.385	62.0	16.05
304.92	1.386	62.1	16.10
304.43	1.387	62.4	16.12
304.43	1.392	62.8	16.13

Table II. (Continued)

Temperature (K)	Pressure (MPa)	Density (kg · m ⁻³)	λ (mW · m ⁻¹ · K ⁻¹)
304.69	3.000	919.9	68.26
304.68	4.000	929.9	69.39
304.82	5.056	938.8	70.52
304.99	5.046	938.1	70.46
304.98	6.000	946.0	71.29
304.97	7.000	953.8	72.16
304.96	8.000	961.0	73.06
304.95	9.000	967.9	73.98
305.26	10.021	973.4	75.02
305.25	11.000	979.4	76.08
305.24	12.000	985.2	76.87
305.23	13.000	990.8	77.79
305.22	14.000	996.1	78.40
305.54	15.113	1000.9	78.93
305.54	16.000	1005.2	79.76
305.53	17.000	1010.0	80.40
305.52	18.000	1014.6	80.94
305.52	19.000	1019.0	81.52
305.51	19.978	1023.2	82.17
305.51	21.000	1027.5	82.70
305.50	22.000	1031.5	83.30
305.50	23.000	1035.4	83.89
305.49	24.000	1039.2	84.59
305.65	25.052	1042.8	85.21
305.48	26.000	1046.6	85.62
305.48	27.000	1050.1	86.12
305.48	28.000	1053.6	86.62
305.47	29.000	1056.9	87.39
305.47	30.038	1060.4	88.03
305.46	31.000	1063.5	88.43
305.62	32.000	1066.3	89.01
305.62	33.000	1069.4	89.54
305.61	34.000	1072.4	90.10
305.61	35.007	1075.4	90.83
305.60	36.000	1078.3	91.20
305.60	37.000	1081.2	91.90
305.59	38.000	1084.0	92.47
305.59	39.000	1086.7	93.19
305.59	39.779	1088.8	93.19
305.58	39.870	1089.1	94.11
305.58	40.000	1089.4	93.78
305.58	41.027	1092.2	94.52
305.58	41.995	1094.7	95.13
305.58	43.038	1097.4	95.59
305.58	44.117	1100.1	96.33
305.56	45.230	1102.9	96.98
305.56	46.003	1104.7	97.62
305.56	47.120	1107.4	98.10
305.55	48.042	1109.6	98.75

by Eq. (3) increase up to $\pm 3\%$ at 600 K and $\pm 6\%$ at 900 K. For the viscosity, the percentage deviations between calculated values using the potential parameters and Eqs. (6) and (9) and extrapolated experimental data fitted by Eq. (5) reach $\pm 3.3\%$ at 600 K and $\pm 13\%$ at 900 K. The agreement with the theory is very satisfactory for viscosity and thermal conductivity in the temperature range where experimental data are available.

4. DENSE FLUID THERMAL CONDUCTIVITY

To determine the excess function or the residual term of the thermal conductivity $\Delta\lambda(T, \rho)$, we performed measurements in the liquid phase and in the supercritical gas phase far away from the critical region along 11 quasi-isotherms, at 306.3, 317.2, 336.5, 348.0, 375.7, 395.1, 414.9, 434.3, 453.8, 473.7, and 498.3 K. The experimental data are reported in Tables II to XII. The densities were calculated with the equation of state reported by Outcalt and McLinden [1]. For the high-density and low-temperature range, we also used the experimental data of Kim et al. [11]. The residual function for the thermal conductivity was represented by a six-order polynomial of the form

$$\frac{\Delta\lambda}{\Lambda_c} = \sum_{i=1}^6 b_i \left(\frac{\rho}{\rho_c} \right)^i \quad (10)$$

where $\rho_c = 432.9 \text{ kg} \cdot \text{m}^{-3}$ is the critical density, the coefficients b_i in Eq. (10) are

$$b_1 = 0.144465, \quad b_2 = 3.60601, \quad b_3 = -7.3279, \quad b_4 = 7.76065$$

$$b_5 = -4.176, \quad b_6 = 1.10242, \quad b_7 = -0.111749$$

and $\Lambda_c = 16.8 \text{ mW} \cdot \text{m}^{-1} \cdot \text{K}^{-1}$.

The excess function of the thermal conductivity is represented as a function of density in Fig. 5 along six-quasi isotherms. Comparisons with the experimental measurements of Yata et al. [12] in the temperature range 268 to 314 K and the pressure range 2.4 to 30.7 MPa show that the corresponding values calculated by the background equation [Eq. (2)] are higher than their data; the relative deviations are within $\pm 6.5\%$ in the density range 890 to $1150 \text{ kg} \cdot \text{m}^{-3}$. Figure 6 shows the relative deviations between calculated values from the background Eq. (2) and the experimental data of Yata as a function of density. In Fig. 7, the deviations between the background equation and experimental data from this work are reported. The deviations are of the order of $\pm 1.5\%$ in the density range 800 to

Table III. Thermal Conductivity of HFC-143a Along the Quasi-Isotherm 317.2 K

Temperature (K)	Pressure (MPa)	Density (kg · m ⁻³)	λ (mW · m ⁻¹ · K ⁻¹)
317.00	2.481	849.8	63.02
316.99	3.000	858.9	63.70
316.97	3.903	872.7	64.83
317.27	5.000	885.6	66.10
317.41	6.023	896.7	67.30
317.40	7.000	906.8	68.25
317.38	7.959	915.9	69.23
317.37	9.000	925.0	70.15
317.36	10.016	933.1	71.20
317.35	11.000	940.5	72.06
317.34	12.000	947.6	72.95
317.33	13.000	954.3	73.80
317.32	14.073	961.0	74.72
317.31	15.000	966.6	75.66
317.30	16.000	972.4	76.42
317.29	17.000	977.8	77.20
317.29	18.100	983.6	77.78
317.28	19.000	988.2	78.44
317.27	20.000	993.1	79.15
317.27	21.000	997.8	79.78
317.27	22.130	1002.9	80.54
317.26	23.000	1006.8	81.27
317.26	24.000	1011.0	81.82
317.25	25.000	1015.2	82.51
317.24	26.148	1019.8	83.10
317.24	27.000	1023.1	83.53
317.23	28.000	1027.0	84.11
317.23	29.000	1031.0	84.75
317.22	30.235	1035.2	85.59
317.23	31.000	1037.9	86.04
317.23	32.000	1041.3	86.41
317.21	33.000	1044.7	87.03
317.23	34.255	1048.8	87.76
317.20	35.000	1051.2	88.05
317.20	36.000	1054.4	88.56
317.20	37.000	1057.5	89.08
317.19	38.400	1061.7	89.91
317.19	39.000	1063.5	90.27
317.19	40.000	1066.5	91.08
317.18	41.400	1070.5	91.54
317.18	42.000	1072.2	91.81
317.17	43.000	1074.9	92.37
317.17	44.300	1078.4	92.82
317.17	45.000	1080.3	93.21
317.16	46.000	1082.9	93.79
317.16	47.000	1085.5	94.37
317.16	48.000	1088.1	94.95
317.16	49.000	1090.6	95.55
317.14	50.000	1093.1	96.15

Table IV. Thermal Conductivity of HFC-143a Along the Quasi-Isotherm 336.5 K

Temperature (K)	Pressure (MPa)	Density (kg · m ⁻³)	λ (mW · m ⁻¹ · K ⁻¹)
336.19	3.551	731.8	56.48
336.18	4.015	752.0	57.22
336.16	4.501	768.6	58.26
336.14	5.000	782.7	59.23
336.11	7.000	823.5	61.09
336.09	7.730	835.0	62.90
336.07	8.911	851.2	64.30
336.49	9.994	862.4	65.72
336.92	11.011	871.7	66.50
336.91	12.200	883.5	67.51
336.90	13.007	890.8	68.60
336.89	14.057	899.8	69.52
336.88	14.915	906.6	70.46
336.87	16.008	914.9	71.27
336.85	16.987	921.8	72.21
336.85	18.031	928.8	72.90
336.85	18.031	928.8	73.01
336.84	19.012	935.1	73.85
336.83	19.944	940.8	74.46
336.82	21.017	947.0	75.28
336.81	22.005	952.5	76.11
336.81	23.008	957.9	76.76
336.80	23.997	963.0	77.33
336.79	24.909	967.6	78.02
336.78	26.027	973.0	78.69
336.78	27.010	977.6	79.29
336.77	28.014	982.1	79.92
336.77	29.015	986.5	80.52
336.77	30.012	990.8	81.17
336.76	31.011	994.9	81.74
336.76	32.005	998.9	82.21
336.75	32.972	1002.7	82.86
336.75	34.003	1006.6	83.35
336.74	34.930	1010.1	84.12
336.74	36.002	1014.0	84.67
336.73	36.997	1017.5	85.19
336.73	37.979	1021.0	85.77
336.72	39.021	1024.5	86.33
336.72	40.393	1029.1	87.16
336.71	41.007	1031.1	87.78
336.71	41.995	1034.2	88.33
336.70	43.012	1037.4	88.80
336.70	44.027	1040.5	89.51
336.69	45.033	1043.5	90.21

Table V. Thermal Conductivity of HFC-143a Along the Quasi-Isotherm 348.0 K

Temperature (K)	Pressure (MPa)	Density (kg · m ⁻³)	λ (mW · m ⁻¹ · K ⁻¹)
348.11	10.002	814.2	62.43
348.10	10.987	827.9	63.66
348.09	12.051	841.0	64.72
348.08	13.016	851.7	65.81
348.08	14.003	861.8	66.79
348.07	15.122	872.3	68.11
348.06	16.007	880.1	68.77
348.06	16.955	887.9	69.85
348.05	18.012	896.1	70.46
348.05	19.037	903.5	71.44
348.05	20.013	910.3	72.10
348.04	21.022	916.9	72.76
348.04	22.036	923.3	73.63
348.03	23.042	929.3	74.40
348.03	24.097	935.4	75.24
348.02	25.093	940.9	76.35
348.02	25.972	945.6	77.06
348.02	27.189	951.9	77.34
348.02	28.013	955.9	78.14
348.01	29.045	960.9	78.64
348.01	30.140	966.0	79.38
348.01	31.006	969.9	79.96
348.01	31.948	974.0	80.49
348.00	33.017	978.6	81.12
348.00	33.779	981.7	81.45
348.00	34.947	986.5	82.39
348.00	36.012	990.7	82.82
348.00	37.131	995.0	83.39
347.99	38.035	998.4	83.84
347.99	38.979	1001.8	84.32
347.99	40.122	1005.9	84.87
347.98	41.230	1009.7	85.77
347.98	42.053	1012.6	86.03
347.98	43.017	1015.8	86.26
347.98	44.012	1019.0	86.50
347.98	44.831	1021.7	86.77
347.98	46.007	1025.4	87.94
347.97	47.043	1028.6	88.23
347.97	48.002	1031.5	88.44

Table VI. Thermal Conductivity of HFC-143a Along the Quasi-Isotherm 375.7 K

Temperature (K)	Pressure (MPa)	Density (kg · m ⁻³)	λ (mW · m ⁻¹ · K ⁻¹)
377.26	0.1013	2.71	21.70
377.25	0.500	13.92	21.96
377.10	1.000	29.00	22.36
377.07	1.500	45.47	22.85
376.91	2.000	63.69	23.35
376.89	2.500	84.00	23.96
376.18	3.000	107.5	24.85
375.72	3.500	134.8	26.14
375.52	4.000	167.2	27.99
375.05	4.500	208.2	30.39
374.83	5.000	260.8	33.61
374.60	5.500	330.6	38.41
374.52	6.000	410.8	43.33
374.48	6.500	482.4	46.33
374.46	7.000	536.7	48.64
374.44	7.500	576.8	50.51
374.42	8.000	607.3	51.74
374.41	8.500	631.8	52.92
374.40	9.000	652.1	53.86
374.39	9.500	669.5	54.78
374.39	10.000	684.7	55.65
374.38	11.000	710.4	56.94
374.36	12.000	731.7	58.43
374.36	13.000	749.9	59.52
374.35	14.000	765.8	60.68
374.34	15.000	780.1	61.86
374.33	16.000	792.9	62.83
374.33	17.000	804.6	63.84
374.32	18.000	815.5	65.14
374.31	19.000	825.5	65.91
374.31	20.000	834.9	66.56
374.30	21.000	843.6	67.45
375.11	22.000	849.7	68.60
375.10	23.000	857.6	69.49
375.10	24.000	865.1	70.40
375.09	25.000	872.2	71.18
375.09	26.000	879.0	71.81
374.28	27.000	887.5	72.34
375.08	28.000	891.8	73.12
375.08	29.000	897.8	73.78

Table VI. (*Continued*)

Temperature (K)	Pressure (MPa)	Density (kg · m ⁻³)	λ (mW · m ⁻¹ · K ⁻¹)
375.07	30.000	903.5	74.47
375.07	31.000	909.1	75.16
375.07	32.000	914.5	75.87
375.07	33.000	919.7	76.40
375.06	34.000	924.7	76.95
374.25	35.000	931.3	77.38
374.25	36.000	936.0	77.94
375.06	37.000	938.9	78.63
375.05	38.000	943.4	79.21
375.05	39.000	947.7	79.80
375.05	40.000	952.0	80.39
375.05	41.000	956.1	80.79
375.04	42.000	960.1	81.20
374.23	43.000	965.6	81.48
374.23	44.000	969.4	81.89
375.04	45.000	971.6	82.44

Table VII. Thermal Conductivity of HFC-143a Along the Quasi-Isotherm 395.1 K

Temperature (K)	Pressure (MPa)	Density (kg · m ⁻³)	λ (mW · m ⁻¹ · K ⁻¹)
396.28	0.1013	2.57	24.18
396.27	0.500	13.17	24.46
396.26	1.000	27.23	24.82
396.24	1.500	42.31	25.16
396.22	2.000	58.60	25.63
395.69	2.500	76.46	26.14
395.66	3.000	95.86	26.84
395.24	3.500	117.5	27.67
395.21	4.000	141.3	28.77
394.78	4.500	168.5	30.17
394.74	5.000	198.7	31.72
394.58	5.500	233.2	33.67
394.39	6.000	272.5	35.89
394.21	6.500	316.2	38.49
394.17	7.000	361.9	41.09
394.13	7.500	407.2	43.68

Table VII. (*Continued*)

Temperature (K)	Pressure (MPa)	Density (kg · m ⁻³)	λ (mW · m ⁻¹ · K ⁻¹)
394.10	8.000	449.1	45.72
394.08	8.500	486.3	47.67
394.07	9.000	518.4	48.96
394.05	9.500	546.0	50.19
394.04	10.000	569.9	51.48
394.02	11.000	609.1	53.36
394.00	12.000	640.2	55.20
393.99	13.000	665.9	56.76
393.98	14.000	687.7	58.23
393.97	15.000	706.7	59.24
393.96	16.000	723.5	60.66
393.96	17.000	738.6	61.67
393.95	18.000	752.3	62.62
393.94	19.000	764.8	63.60
393.94	20.000	776.4	64.36
393.93	21.000	787.1	65.14
393.93	22.000	797.1	65.83
393.92	23.000	806.6	66.92
393.92	24.000	815.4	67.61
393.91	25.000	823.8	68.32
393.91	26.000	831.8	69.05
393.91	27.000	839.4	69.79
393.90	28.000	846.7	70.54
393.90	29.000	853.6	71.00
393.89	30.000	860.2	71.78
393.89	31.000	866.6	72.42
393.89	32.000	872.7	73.07
393.88	33.000	878.6	73.73
393.88	34.000	884.4	74.40
393.88	35.000	889.9	75.18
393.88	36.000	895.2	75.60
393.87	37.000	900.4	76.13
393.87	38.000	905.4	76.75
393.87	39.000	910.3	77.29
393.87	40.000	915.0	77.84
393.86	41.000	919.6	78.40
393.86	42.000	924.1	78.97
393.86	43.000	928.4	79.54
393.86	44.000	932.7	79.93
393.86	45.000	936.9	80.32

Table VIII. Thermal Conductivity of HFC-143a Along the Quasi-Isotherm 414.9 K

Temperature (K)	Pressure (MPa)	Density (kg · m ⁻³)	λ (mW · m ⁻¹ · K ⁻¹)
416.02	0.1013	2.45	25.72
416.01	0.500	12.48	26.02
415.99	1.000	25.65	26.52
415.97	1.500	39.60	27.04
415.95	2.000	54.42	27.57
415.31	2.500	70.38	28.12
415.29	3.000	87.33	28.73
415.02	3.500	105.6	29.41
414.75	4.000	125.4	30.03
414.73	4.500	146.5	30.89
414.45	5.000	169.5	31.80
414.17	5.500	194.5	33.01
414.01	6.000	221.3	34.60
413.85	6.500	250.0	36.03
413.84	7.000	280.1	37.42
413.55	7.500	312.4	38.98
413.52	8.000	344.5	40.79
413.37	8.500	376.8	42.51
413.22	9.000	408.2	44.20
413.20	9.500	437.2	45.71
413.19	10.000	464.0	46.97
413.16	11.000	511.0	48.90
413.15	12.000	550.0	50.97
413.13	13.000	582.5	52.83
413.11	14.000	610.1	54.43
413.10	15.000	633.8	55.93
413.09	16.000	654.7	57.01
413.09	17.000	673.2	58.13
413.07	18.000	689.8	58.97
413.07	19.000	704.9	59.89
413.06	20.000	718.8	60.79
413.06	21.000	731.6	61.65
413.81	22.000	741.3	62.89
413.80	23.000	752.4	63.87
413.79	24.000	762.8	64.88
413.79	25.000	772.7	65.79
413.78	26.000	781.9	66.59
413.78	27.000	790.7	67.41
413.77	28.000	799.0	68.25
413.77	29.000	807.0	69.11

Table VIII. (*Continued*)

Temperature (K)	Pressure (MPa)	Density (kg · m ⁻³)	λ (mW · m ⁻¹ · K ⁻¹)
413.76	30.000	814.6	69.91
413.76	31.000	821.9	70.51
413.76	32.000	828.9	71.11
413.75	33.000	835.5	71.89
413.75	34.000	842.0	72.56
413.75	35.000	848.2	73.17
413.74	36.000	854.2	73.82
413.74	37.000	860.0	74.49
413.74	38.000	865.6	75.00
413.74	39.000	871.1	75.51
413.74	40.000	876.3	76.03
413.73	41.000	881.5	76.56
413.73	42.000	886.4	77.10
413.73	43.000	891.3	77.64
413.72	44.000	896.0	78.19
413.72	45.000	900.6	78.75

Table IX. Thermal Conductivity of HFC-143a Along the Quasi-Isotherm 434.3 K

Temperature (K)	Pressure (MPa)	Density (kg · m ⁻³)	λ (mW · m ⁻¹ · K ⁻¹)
435.05	0.1013	2.34	27.99
435.04	0.500	11.88	28.33
435.03	1.000	24.32	28.72
435.02	1.500	37.36	29.18
435.00	2.000	51.06	29.62
434.63	2.500	65.56	30.01
434.61	3.000	80.77	30.50
434.36	3.500	96.92	30.98
434.34	4.000	113.9	31.56
434.32	4.500	131.8	32.34
434.06	5.000	150.9	33.15
434.04	5.500	170.8	34.00
433.78	6.000	192.0	34.74
433.63	6.500	214.1	35.88
433.61	7.000	237.0	36.96
433.47	7.500	260.9	38.07

Table IX. (*Continued*)

Temperature (K)	Pressure (MPa)	Density (kg · m ⁻³)	λ (mW · m ⁻¹ · K ⁻¹)
433.45	8.000	285.1	39.22
433.43	8.500	309.7	40.41
433.43	9.000	334.3	41.70
433.40	9.500	358.6	42.81
433.26	10.000	382.7	43.88
433.24	11.000	427.4	45.98
433.22	12.000	467.5	47.96
433.20	13.000	502.8	49.94
433.18	14.000	533.8	51.50
433.17	15.000	561.1	53.01
433.15	16.000	585.2	54.51
433.14	17.000	606.7	55.81
433.13	18.000	626.1	56.88
433.13	19.000	643.6	57.99
433.12	20.000	659.7	59.13
433.11	21.000	674.4	60.25
433.10	22.000	688.1	61.20
433.10	23.000	700.8	62.13
433.09	24.000	712.6	62.96
433.09	25.000	723.8	63.81
433.08	26.000	734.2	64.56
433.08	27.000	744.2	65.32
433.07	28.000	753.6	66.24
433.07	29.000	762.5	67.04
433.55	30.000	769.9	68.34
433.55	31.000	778.0	68.90
433.55	32.000	785.8	69.48
433.54	33.000	793.3	70.06
433.54	34.000	800.5	70.66
433.54	35.000	807.4	71.26
433.54	36.000	814.1	71.87
433.53	37.000	820.5	72.50
433.53	38.000	826.7	73.14
433.52	39.000	832.7	73.78
433.52	40.000	838.5	74.44
433.52	41.000	844.2	74.94
433.52	42.000	849.6	75.45
433.52	43.000	854.9	75.96
433.51	44.000	860.1	76.48
433.51	45.000	865.1	77.01

Table X. Thermal Conductivity of HFC-143a Along the Quasi-Isotherm 453.8 K

Temperature (K)	Pressure (MPa)	Density (kg · m ⁻³)	λ (mW · m ⁻¹ · K ⁻¹)
454.71	0.1013	2.24	30.15
454.71	0.500	11.33	30.41
454.70	1.000	23.10	30.68
454.69	1.500	35.35	30.99
454.68	2.000	48.10	31.39
454.43	2.500	61.43	31.82
454.42	3.000	75.30	32.28
454.41	3.500	89.76	32.82
454.16	4.000	104.9	33.29
454.15	4.500	120.7	33.86
454.02	5.000	137.1	34.33
454.13	5.500	154.0	35.00
455.00	6.000	171.8	35.63
453.74	6.500	190.2	36.40
453.61	7.000	209.1	37.15
453.46	7.500	228.6	38.93
453.46	8.000	248.2	38.89
453.44	8.500	268.2	39.91
453.31	9.000	288.5	40.83
453.30	9.500	308.6	41.85
453.28	10.000	328.6	42.84
453.14	11.000	367.8	44.63
453.00	12.000	404.9	46.49
452.98	13.000	439.0	48.07
452.97	14.000	470.1	49.59
452.95	15.000	498.3	51.15
452.94	16.000	523.8	52.56
452.93	17.000	546.9	53.95
452.91	18.000	567.9	55.23
452.91	19.000	587.1	56.36
452.90	20.000	604.8	57.44
452.89	21.000	621.1	58.58
452.88	22.000	636.1	59.43
452.88	23.000	650.2	60.30
452.87	24.000	663.3	61.30
452.86	25.000	675.6	62.11
452.86	26.000	687.2	63.06
452.85	27.000	698.1	63.77
452.85	28.000	708.5	64.92
452.84	29.000	718.3	65.69

Table X. (Continued)

Temperature (K)	Pressure (MPa)	Density (kg · m ⁻³)	λ (mW · m ⁻¹ · K ⁻¹)
452.84	30.000	727.7	66.66
452.83	31.000	736.6	67.58
452.83	32.000	745.2	68.17
452.83	33.000	753.4	68.88
452.82	34.000	761.2	69.60
452.82	35.000	768.8	70.30
452.82	36.000	776.0	70.90
452.81	37.000	783.0	71.51
452.81	38.000	789.8	72.09
452.81	39.000	796.3	72.72
452.80	40.000	802.6	73.22
452.80	41.000	808.7	73.70
452.80	42.000	814.6	74.19
452.80	43.000	820.4	74.69
452.80	44.000	826.0	75.20
452.79	45.000	831.4	75.71

Table XI. Thermal Conductivity of HFC-143a Along the Quasi-Isotherm 473.7 K

Temperature (K)	Pressure (MPa)	Density (kg · m ⁻³)	λ (mW · m ⁻¹ · K ⁻¹)
474.42	0.1013	2.14	32.23
474.42	0.500	10.82	32.43
474.41	1.000	22.01	32.67
474.41	1.500	33.57	32.94
474.40	2.000	45.52	33.25
474.28	2.500	57.90	33.67
474.39	3.000	70.67	34.04
474.38	3.500	83.90	34.48
474.01	4.000	97.69	34.96
473.65	4.500	112.0	35.41
473.64	5.000	126.6	35.93
473.52	5.500	141.7	36.46
473.39	6.000	157.3	37.01
473.26	6.500	173.3	37.60
473.25	7.000	189.5	38.18
473.24	7.500	206.0	38.83

Table XI. (*Continued*)

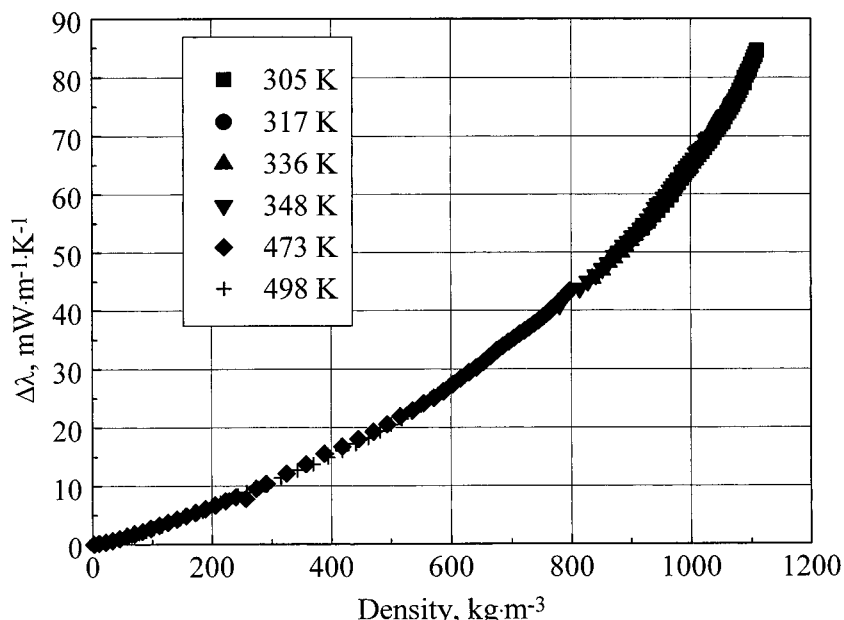
Temperature (K)	Pressure (MPa)	Density (kg · m ⁻³)	λ (mW · m ⁻¹ · K ⁻¹)
473.23	8.000	222.8	39.53
473.22	8.500	239.8	40.22
473.23	9.000	256.9	39.93
473.20	9.500	274.1	41.68
473.19	10.000	291.2	42.51
473.17	11.000	325.0	44.28
473.15	12.000	357.7	45.90
473.13	13.000	388.9	47.71
473.00	14.000	418.5	48.89
472.99	15.000	445.8	50.16
472.98	16.000	471.1	51.42
472.97	17.000	494.5	52.66
472.95	18.000	516.1	54.05
472.95	19.000	536.0	55.04
472.94	20.000	554.5	56.27
472.93	21.000	571.7	57.14
473.16	22.000	587.2	58.28
473.15	23.000	602.1	59.44
473.14	24.000	616.2	60.52
473.13	25.000	629.4	61.54
473.13	26.000	641.8	62.35
473.12	27.000	653.6	63.30
473.12	28.000	664.8	64.28
473.11	29.000	675.4	65.29
473.11	30.000	685.5	66.07
473.10	31.000	695.1	66.73
473.10	32.000	704.3	67.41
473.10	33.000	713.1	68.10
473.10	34.000	721.6	68.66
473.10	35.000	729.7	69.23
473.09	36.000	737.5	69.81
473.08	37.000	745.1	70.40
473.08	38.000	752.4	71.00
473.08	39.000	759.4	71.61
473.08	40.000	766.2	72.23
473.07	41.000	772.8	72.87
473.07	42.000	779.1	73.51
473.07	43.000	785.3	74.16
473.06	44.000	791.3	74.82
473.06	45.000	797.1	75.50

Table XII. Thermal Conductivity of HFC-143a Along the Quasi-Isotherm 498.3 K

Temperature (K)	Pressure (MPa)	Density (kg · m ⁻³)	λ (mW · m ⁻¹ · K ⁻¹)
499.02	0.1013	2.03	34.95
499.01	0.500	10.26	35.11
499.01	1.000	20.80	35.26
499.01	1.500	31.62	35.50
499.00	2.000	42.73	35.82
498.88	2.500	54.16	36.18
498.88	3.000	65.89	36.38
498.87	3.500	77.93	36.76
498.75	4.000	90.31	37.21
498.63	4.500	103.0	37.64
498.62	5.000	116.0	37.99
498.61	5.500	129.3	38.54
498.49	6.000	142.8	39.12
498.60	6.500	156.6	39.58
498.59	7.000	170.6	40.07
498.58	7.500	184.7	40.45
497.89	8.000	199.6	41.32
497.88	8.500	214.2	41.91
497.87	9.000	228.8	42.46
497.86	9.500	243.4	43.13
497.86	10.000	258.0	43.71
497.84	11.000	287.0	44.92
497.83	12.000	315.5	46.19
497.81	13.000	343.1	47.46
497.80	14.000	369.7	48.55
497.79	15.000	394.9	49.73
497.78	16.000	418.8	50.89
497.77	17.000	441.3	52.01
497.76	18.000	462.4	53.02
497.75	19.000	482.3	54.15
497.74	20.000	500.9	55.24
497.73	21.000	518.4	56.28
497.73	22.000	534.8	57.42
497.72	23.000	550.3	58.54
497.71	24.000	564.9	59.59
497.71	25.000	578.7	60.45
497.70	26.000	591.8	61.35
497.69	27.000	604.2	62.50
497.69	28.000	616.1	63.45
497.68	29.000	627.3	64.19

Table XII. (Continued)

Temperature (K)	Pressure (MPa)	Density (kg · m ⁻³)	λ (mW · m ⁻¹ · K ⁻¹)
497.68	30.000	638.0	64.90
497.67	31.000	648.3	65.67
497.67	32.000	658.1	66.45
497.67	33.000	667.5	67.12
497.66	34.000	676.6	67.80
497.66	35.000	685.3	68.50
497.66	36.000	693.6	69.21
497.65	37.000	701.7	69.79
497.65	38.000	709.5	70.47
497.65	39.000	717.0	71.06
497.64	40.000	724.3	71.67
497.64	41.000	731.4	72.14
497.64	42.000	738.2	72.60
497.64	43.000	744.8	73.08
497.64	44.000	751.3	73.56
497.63	45.000	757.5	74.05

**Fig. 5.** The excess function of thermal conductivity along six quasi-isotherms.

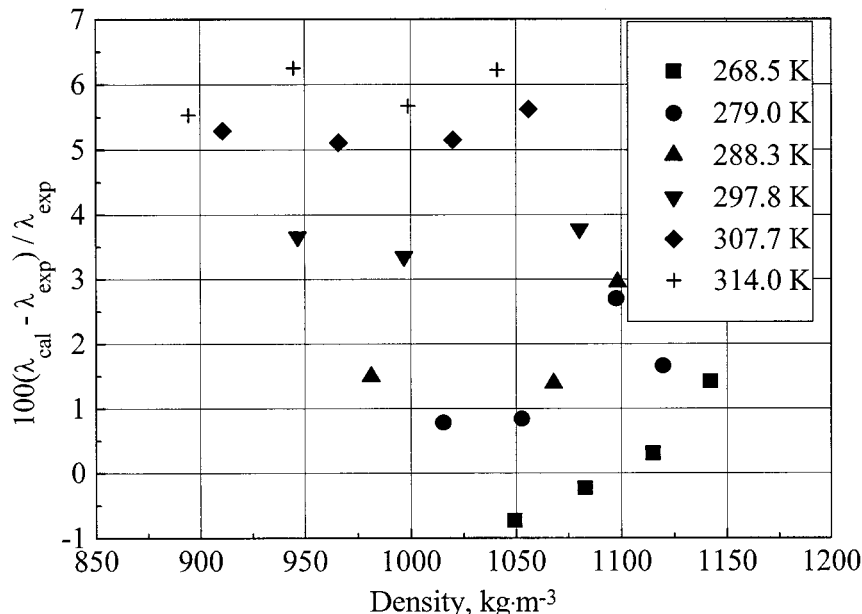


Fig. 6. Relative deviations between the values calculated by the background equation [Eq. (2)] and the experimental data of Yata et al. [12].

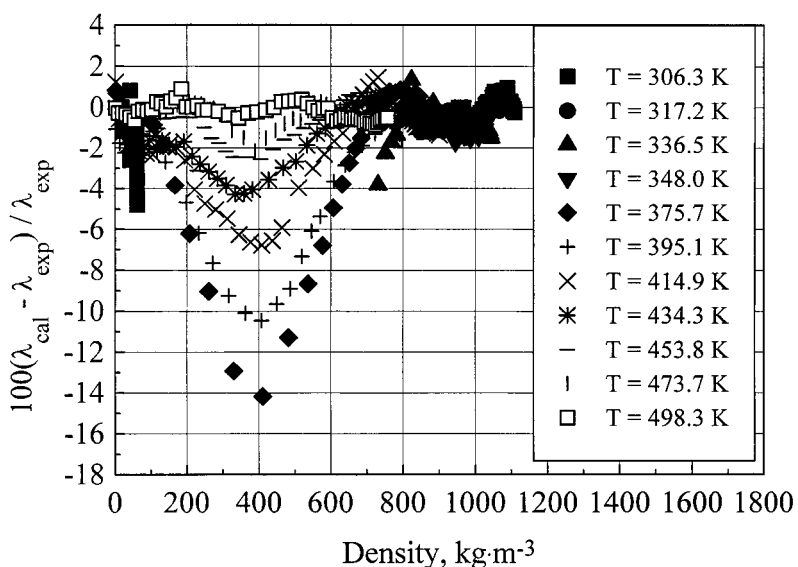


Fig. 7. Relative deviations between the calculated values of thermal conductivity by the background equation [Eq. (2)] and experimental data from this work.

1100 kg · m⁻³. The larger deviations observed at lower densities, which are maximum at the critical density, correspond to the critical enhancement.

5. CONCLUSION

New measurements of the thermal conductivity of HFC-143a are presented in the temperature range from 300 to 500 K along 11 quasi-isotherms and at pressures up to 50 MPa with an estimated uncertainty of $\pm 1.5\%$. At atmospheric pressure, large discrepancies were observed with available experimental data, however, rather good agreement was found with the dilute gas theory of Chapman–Enskog, which corroborates the accuracy of our experimental data. A background equation was determined which can be used to calculate the thermal conductivity from 260 to 600 K and up to a density of 1150 kg · m⁻³ with an uncertainty of $\pm 3\%$. In the critical region and in the gas below the saturation curve, supplementary functional forms must be added to take into account, respectively, the critical enhancement and the approach of the gas–liquid transition.

ACKNOWLEDGMENT

We are indebted to Atochem for providing us HFC-143a samples.

REFERENCES

1. S. L. Outcalt and M. O. McLinden, *Int. J. Thermophys.* **18**:1448 (1997).
2. A. T. Sousa, P. S. Fialho, C. A. Nieto de Castro, R. Tufeu, and B. Le Neindre, *Int. J. Thermophys.* **13**:363 (1992).
3. B. Le Neindre and Y. Garrabos, *Int. J. Thermophys.* **20**:375 (1999).
4. B. Le Neindre and Y. Garrabos, *Int. J. Thermophys.* **20**:1379 (1999).
5. B. Le Neindre and R. Tufeu, in *Experimental Thermodynamics III. Measurements of the Transport Properties of Fluids*, W. A. Wakeham, A. Nagashima, and J. V. Sengers, eds. (Blackwell, Oxford, 1991), pp. 111–142.
6. U. Hammerschmidt, *Int. J. Thermophys.* **16**:1203 (1995).
7. Y. Tanaka, M. Nakata, and T. Makita, *Int. J. Thermophys.* **12**:949 (1991).
8. Y. Takahashi, N. Shibasaki-Kitakawa, and C. Yokoyama, *Int. J. Thermophys.* **20**:435 (1999).
9. A. Yokozeki, H. Sato, and K. Watanabe, *Int. J. Thermophys.* **19**:89 (1998).
10. J. Kestin, K. Knierim, E. A. Mason, B. Najafi, S. T. Ro, and M. Waldam, *J. Phys. Chem. Ref. Data* **13**:229 (1984).
11. M. S. Kim, personal communication (Seoul National University, Seoul, Korea).
12. J. Yata, M. Hori, K. Kobayashi, and T. Minamiyama, *Int. J. Thermophys.* **17**:561 (1996).